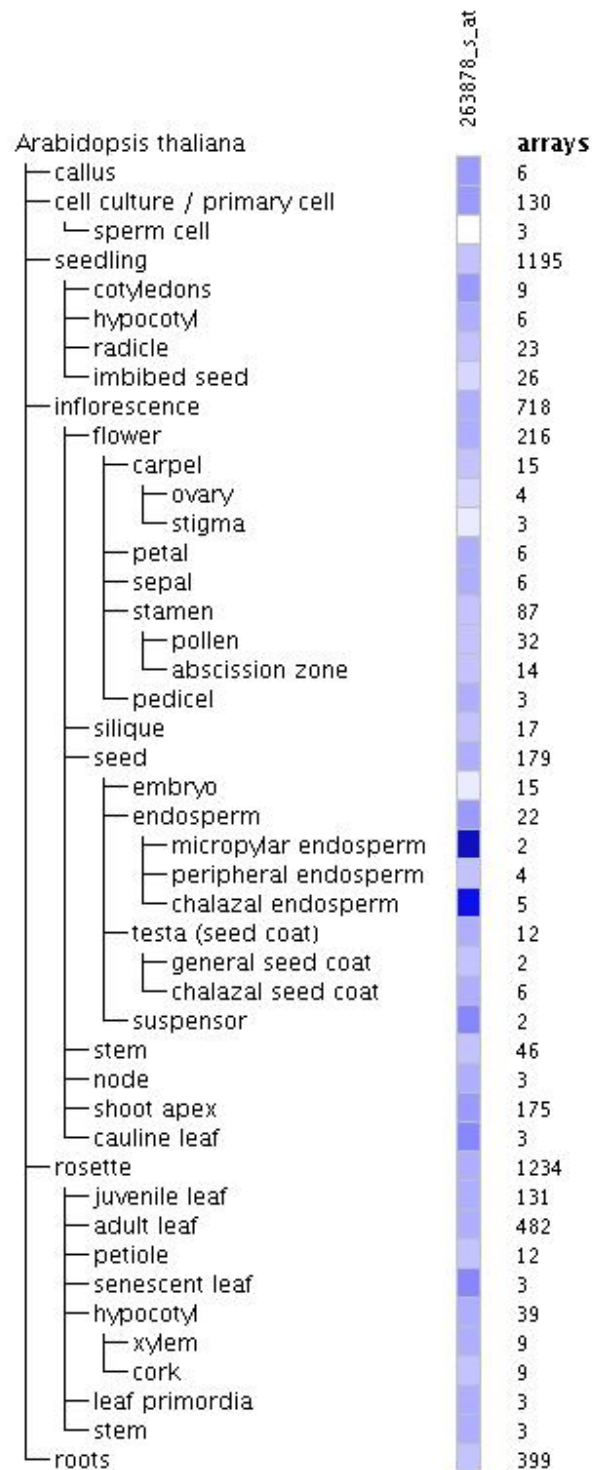**Supplemental Figure 1:** Alignment of plants, yeast and human LST8 protein sequences. Predicted turns and loops are, respectively, shown on top in red and blue. Each WD 40 repeat contains four β strands (Sa to Sd) which are only shown for the beginning and the end of the sequences. Conserved residues are shown in red.

263878_s_at

Arabidopsis thaliana		arrays
callus		6
cell culture / primary cell		130
sperm cell		3
seedling		1195
cotyledons		9
hypocotyl		6
radicle		23
imbibed seed		26
inflorescence		718
flower		216
carpel		15
ovary		4
stigma		3
petal		6
sepal		6
stamen		87
pollen		32
abscission zone		14
pedicel		3
silique		17
seed		179
embryo		15
endosperm		22
micropylar endosperm		2
peripheral endosperm		4
chalazal endosperm		5
testa (seed coat)		12
general seed coat		2
chalazal seed coat		6
suspensor		2
stem		46
node		3
shoot apex		175
cauline leaf		3
rosette		1234
juvenile leaf		131
adult leaf		482
petiole		12
senescent leaf		3
hypocotyl		39
xylem		9
cork		9
leaf primordia		3
stem		3
roots		399

Supplemental Figure 2 : Expression of the Arabidopsis *LST8* genes in various organs. The expression level is correlated to the intensity of the color. Data are from the Genevestigator website (genevestigator.com).

2

Supplemental Figure 3 : GUS staining of a transformed Arabidopsis plants carrying
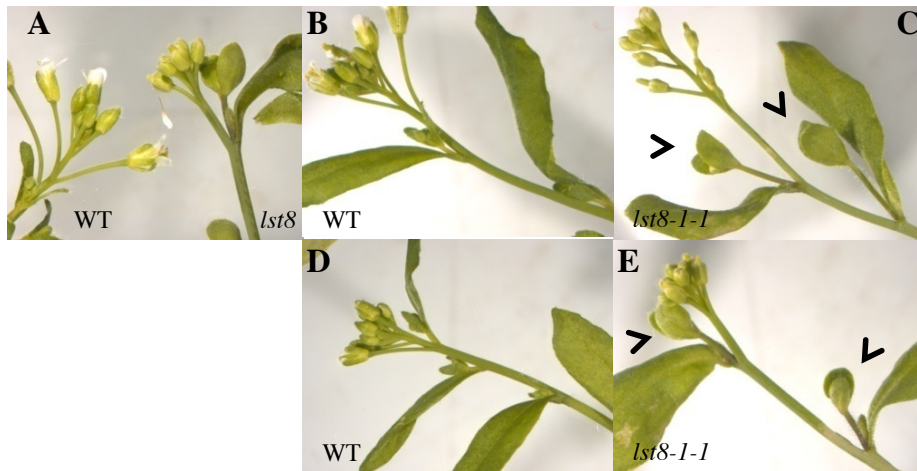a pLst8:*GUS* construct containing 1kb of *LST8-1* promoter. Reconstitution of a stained inflorescence.
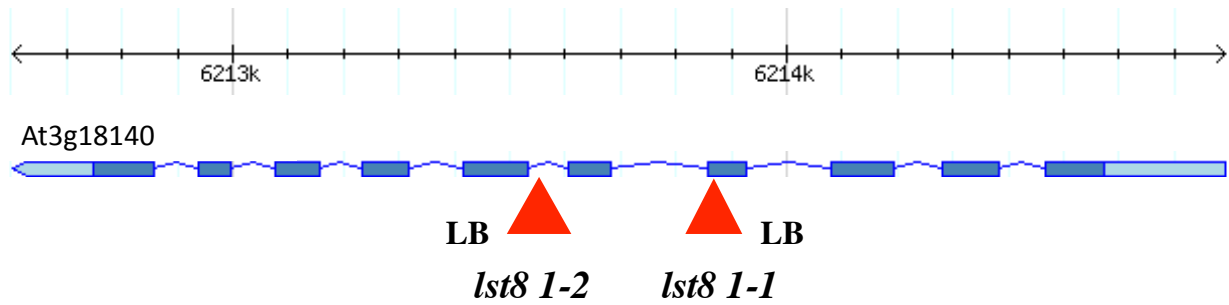
**Supplemental Figure 4** : Position of the T-DNA insertions in the *lst8-1* mutants.
LB indicates the left borders of the inserted T-DNAs.
lst8-1-1: Salk collection
*lst8-1-2*: Sail collection

Supplemental Figure 5 : Mutations in *LST8-1* gene affect stem and flower bud morphology and organization. (A) *lst8-1-1* mutant on the right fails to develop normal flowers compared to the WT on the left. Flowers formed by *lst8-1-1* mutant stay small and unexpanded (C, E) compared to WT ones (B, D). Moreover axillary buds in *lst8-1-1* mutant inflorescence appear larger and emerging stems are longer and more developed (C, E, black arrows) compared to WT (B, D).
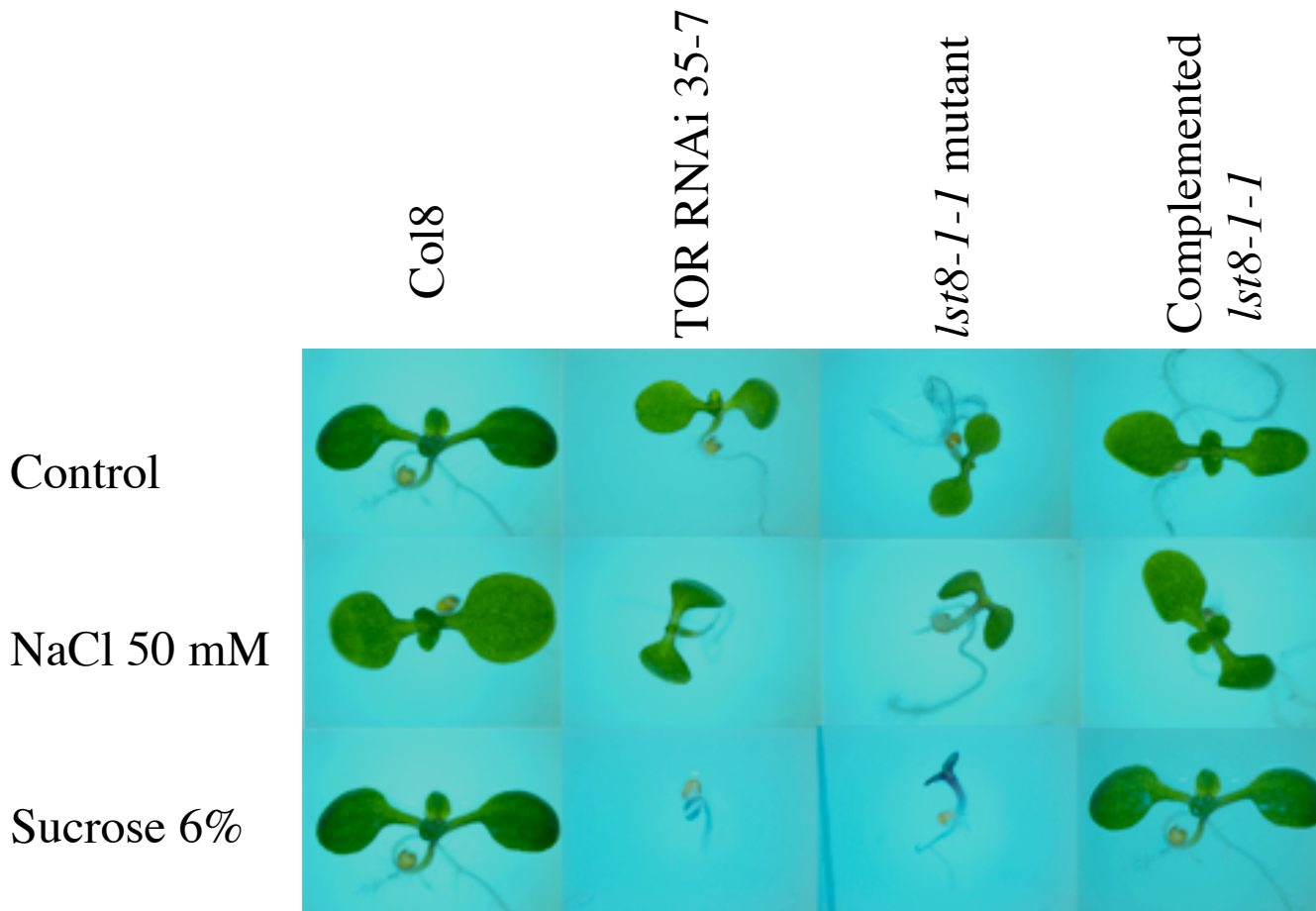
Supplemental Figure 8 : Germinating plantlets from the *lst8-1* mutant line display the same sensitivity to high sugar concentrations as a TOR RNAi line.

Seeds from the *lst8-1-1* mutant were sown in vitro on MS/2 medium and grown for 8 days in long day conditions with seeds from the TOR RNAi line 35-7 and a complemented *lst8-1-1* mutant.

The *lst8-1-1* mutant was complemented by pLst8:Lst8 cDNA construct (see Methods for details).
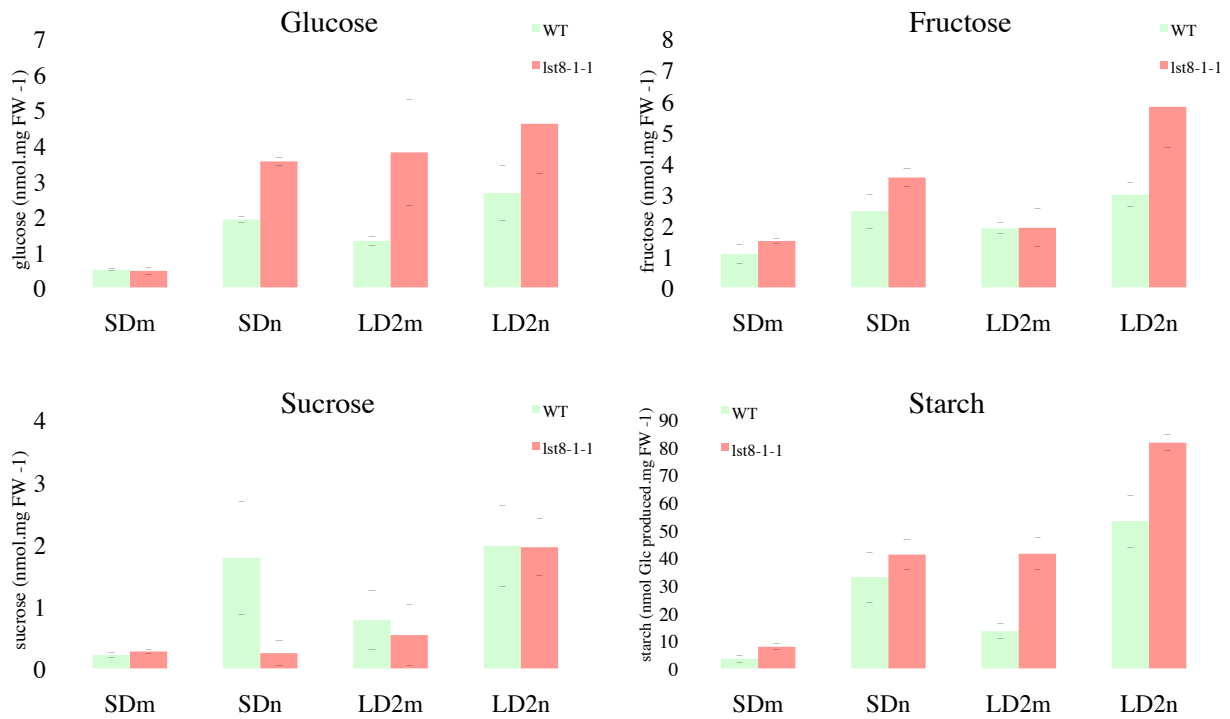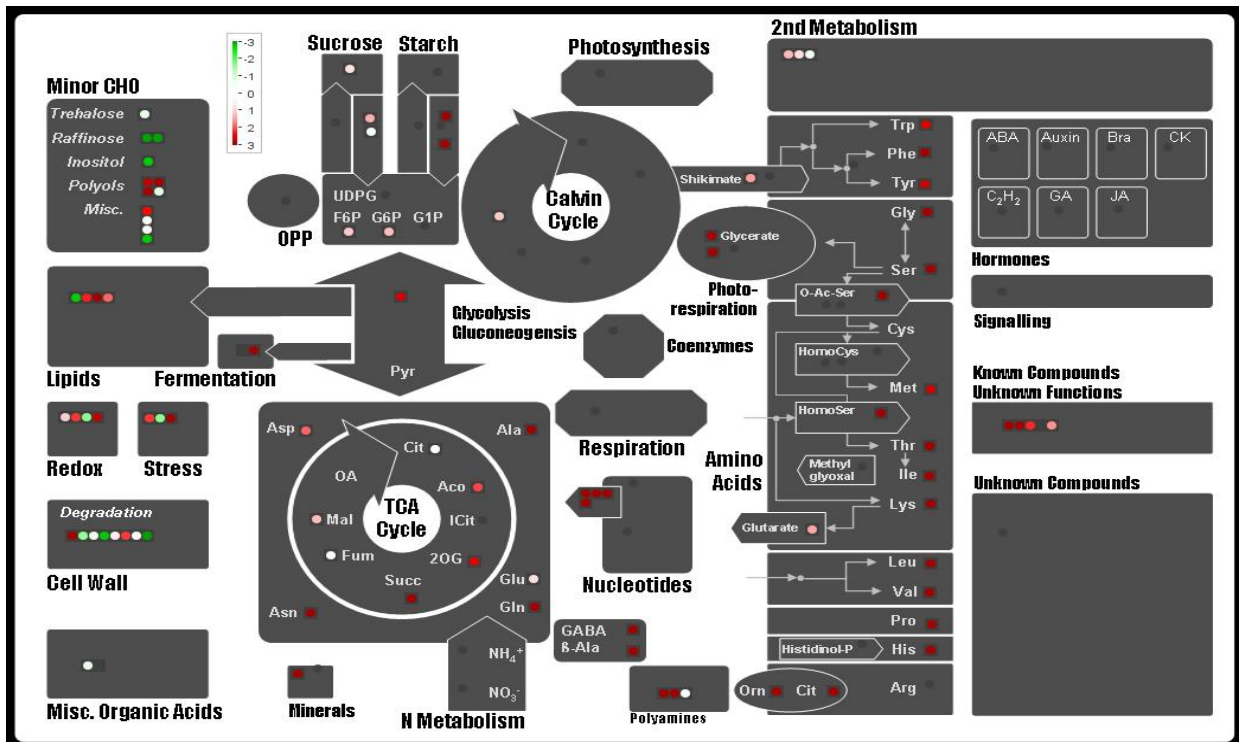
Supplemental Figure 9 : Diurnal variations in sugar and starch contents during the transition
from short days (SD) to long days (LD) in the wild-type (WT) and in the *lst8-1-1* mutant.
Plants were first grown in controlled SD conditions and harvested at the beginning
(morning, m) and end (night, n) of the day preceding the shift to LD. Plants were again harvested
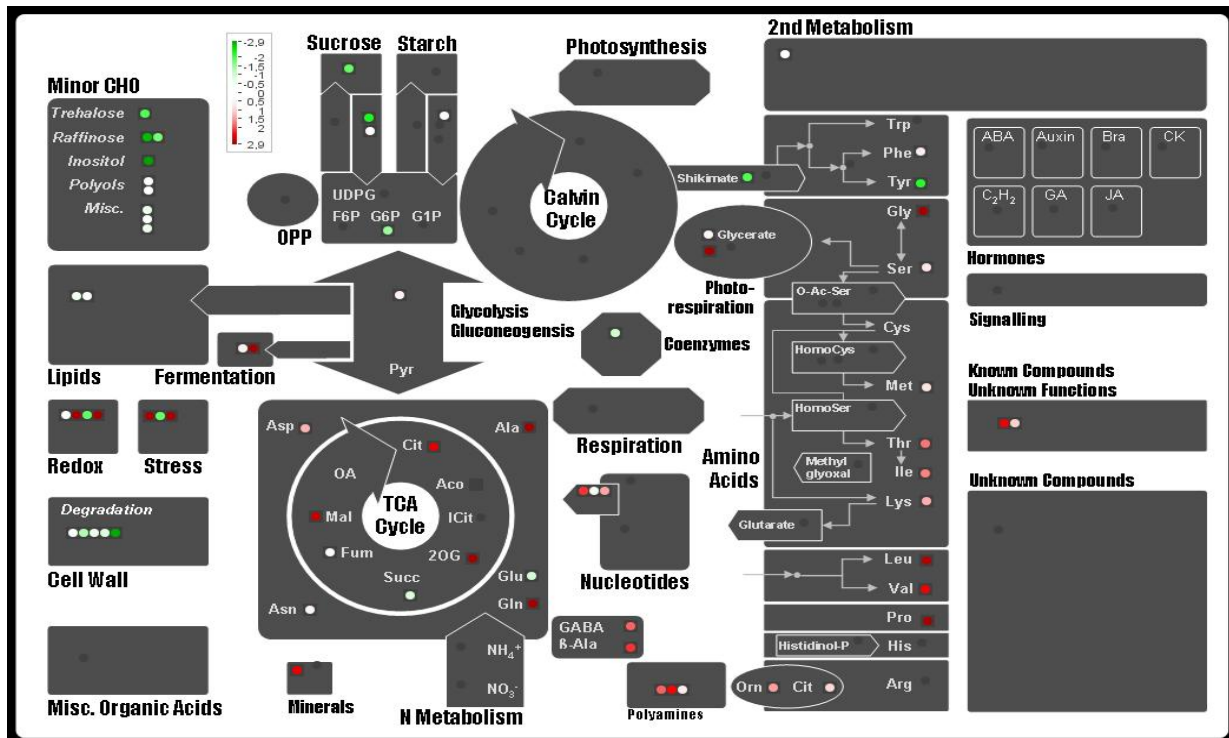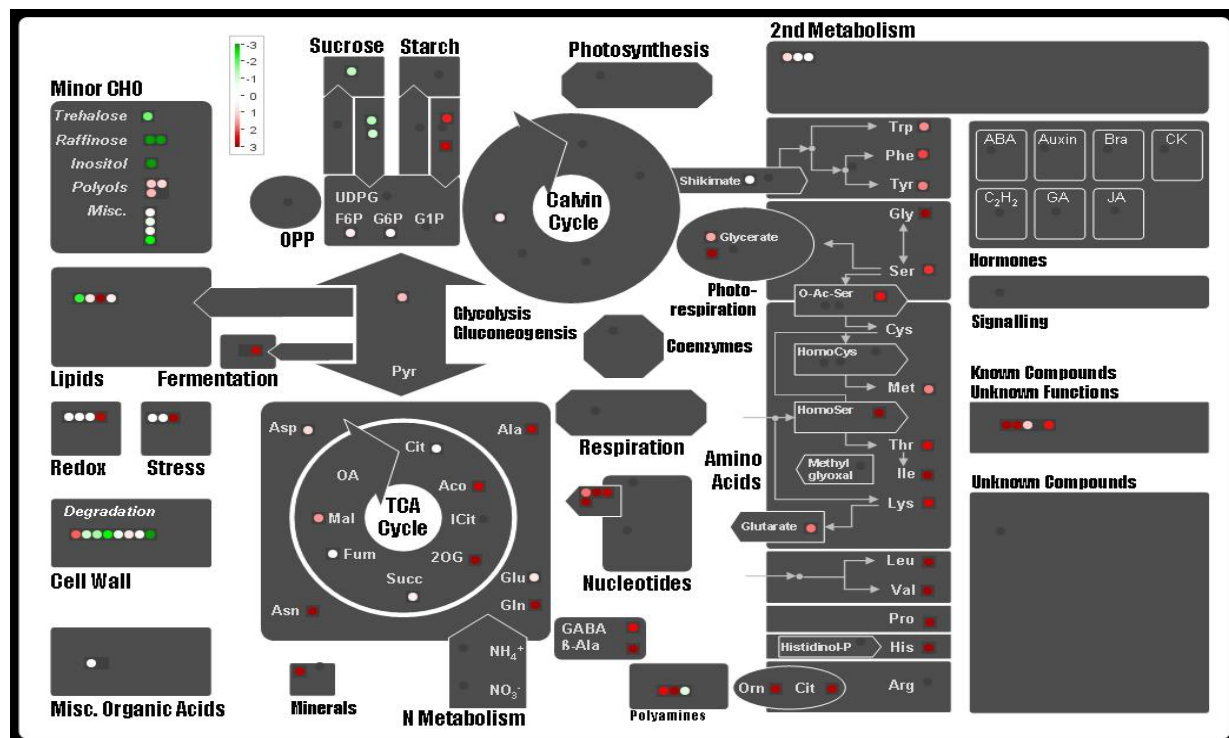at day two after the start of LD conditions. Results are mean of at least three different samples ± SD

A

B
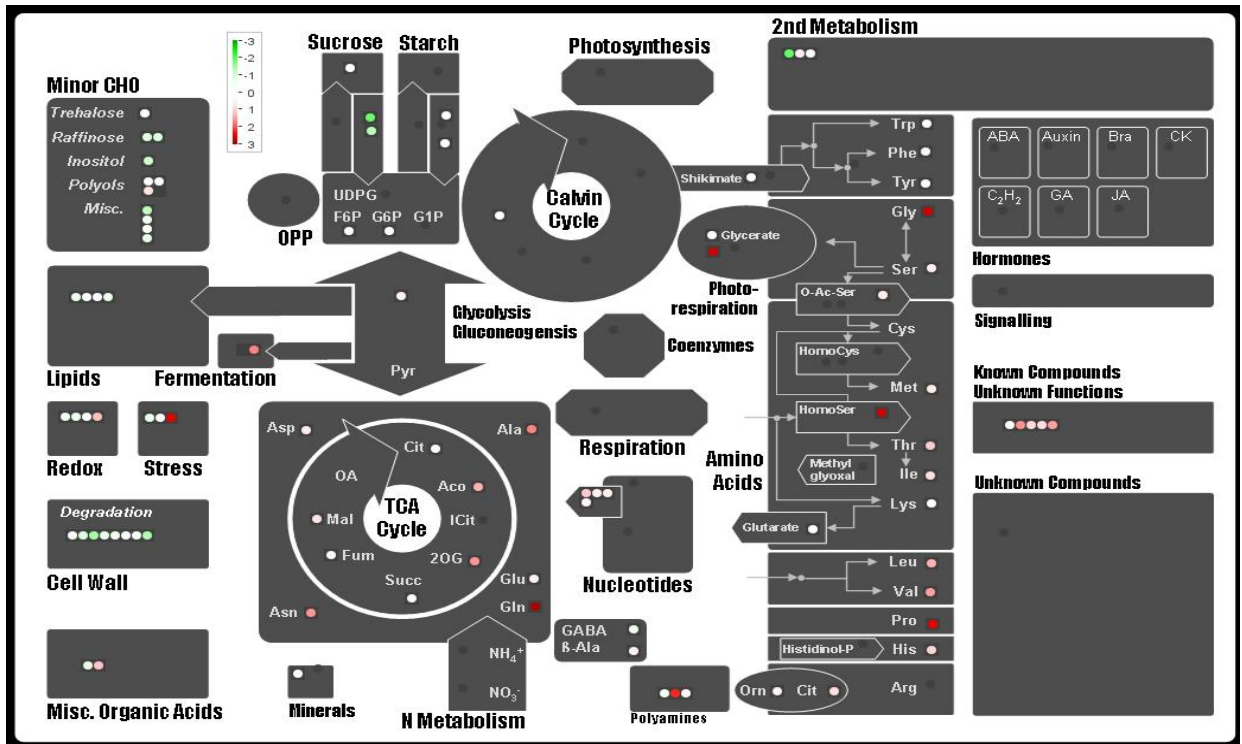
Supplemental Figure : : Mapman representations of metabolite variations in *lst8-1-2* mutants using global GC-MS analysis. Leaves from the *lst8-1-2* mutants were collected from (A) short-day grown plants or (B) after transfer to long-day conditions for 12 days and relative metabolite accumulations were compared with WT plants grown in the same conditions. '':

Supplemental Figure 9:
Variations in metabolite levels in *lst8-1-2* mutants
and WT plants exposed to long days.
Samples and metabolites were clustered. The color scale shows
the concentrations ratios in log2.

JL+06M: *lst8-1-2* mutant after 6 days of transfer to long-
days conditions (triplicate)
JL+01M: same after one day of transfer to long-
days conditions (triplicate)
JC_M: *lst8-1-2* mutant grown in short-days conditions
JL+01C, JL+06C, JC_C: same as above for the WT control
plants (triplicate).

9

A

B

Supplemental Figure 10 : Mapman representations of global metabolite analysis using GC-MS in *lst8-1* mutants.
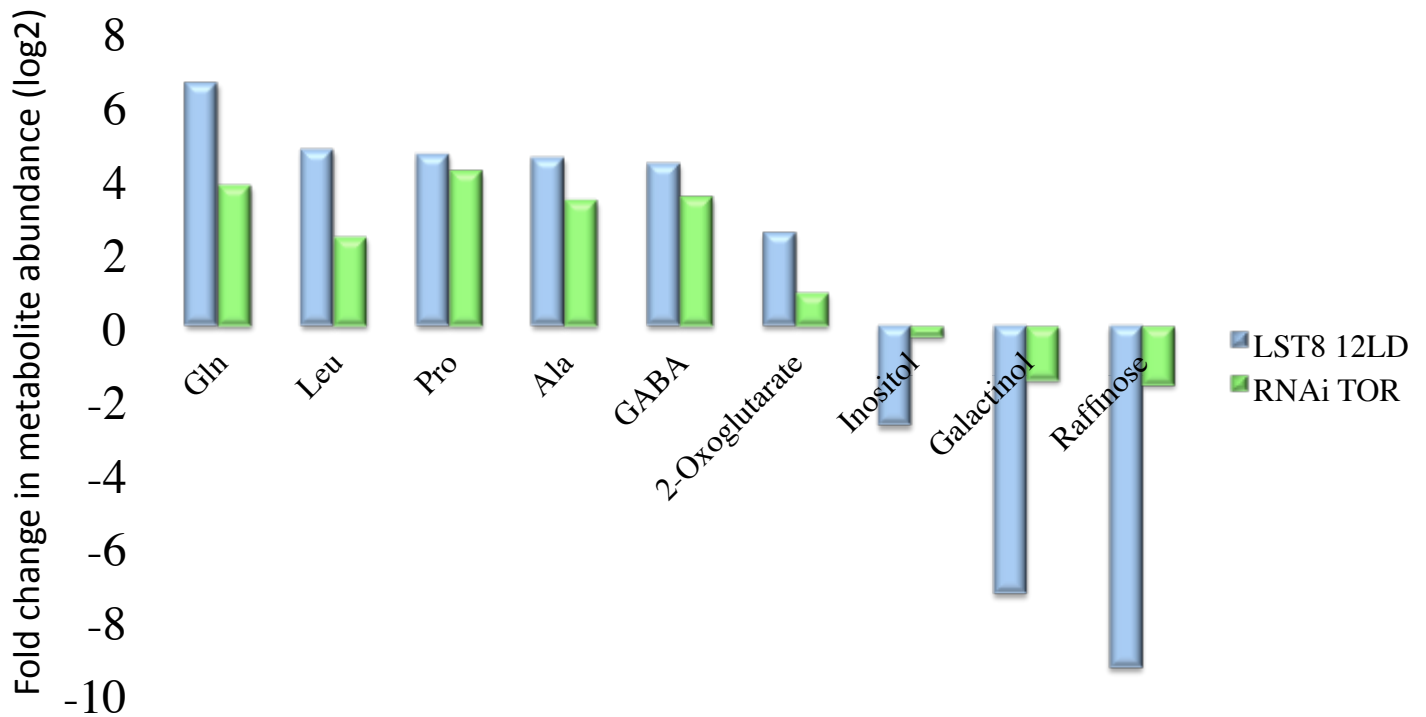
Rosettes from the *lst8-1* mutants were collected after transfer to long-day conditions for 6 days and relative metabolite accumulation was compared with WT plants grown in the same conditions.

A: *lst8-1-1* mutant; B: *lst8-1-2* mutant.
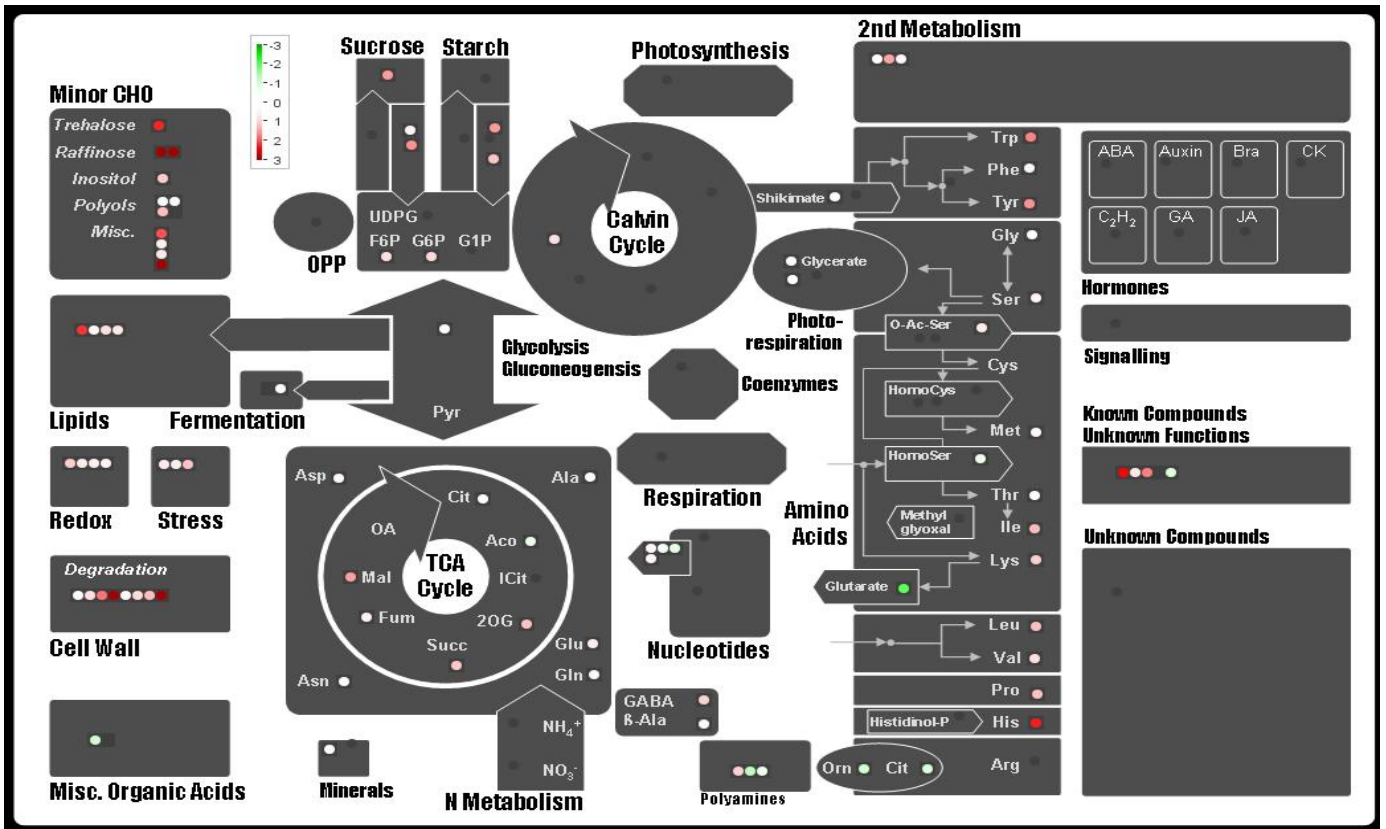
Supplemental Figure 11: Mapman representations of global metabolite analysis using GC-MS in WT plants.

Leaves from the WT plants were collected after transfer to long-day conditions for 6 days and relative metabolite accumulation was compared with WT plants grown in short days.

Supplemental Figure 12: Changes in metabolite accumulations determined by GC-MS in the *lst8-1-2* mutant and in TOR inducible RNAi lines.

LST8 12LD: Leaves from the *lst8-1-2* mutant plants were collected after transfer to long-day conditions for 12 days and relative accumulations were compared for some metabolites with WT plants grown in the same conditions (see Figure 12 for details).

RNAi TOR: The two independent inducible TOR RNAi lines were induced with ethanol for 2 days and relative metabolite accumulation was compared with control plants grown in the same conditions (see Methods for details). Galactinol and raffinose were measured in dark-grown plantlets sown on ethanol. Ratio were obtained from the means of three independent samples for each of the two RNAi lines.
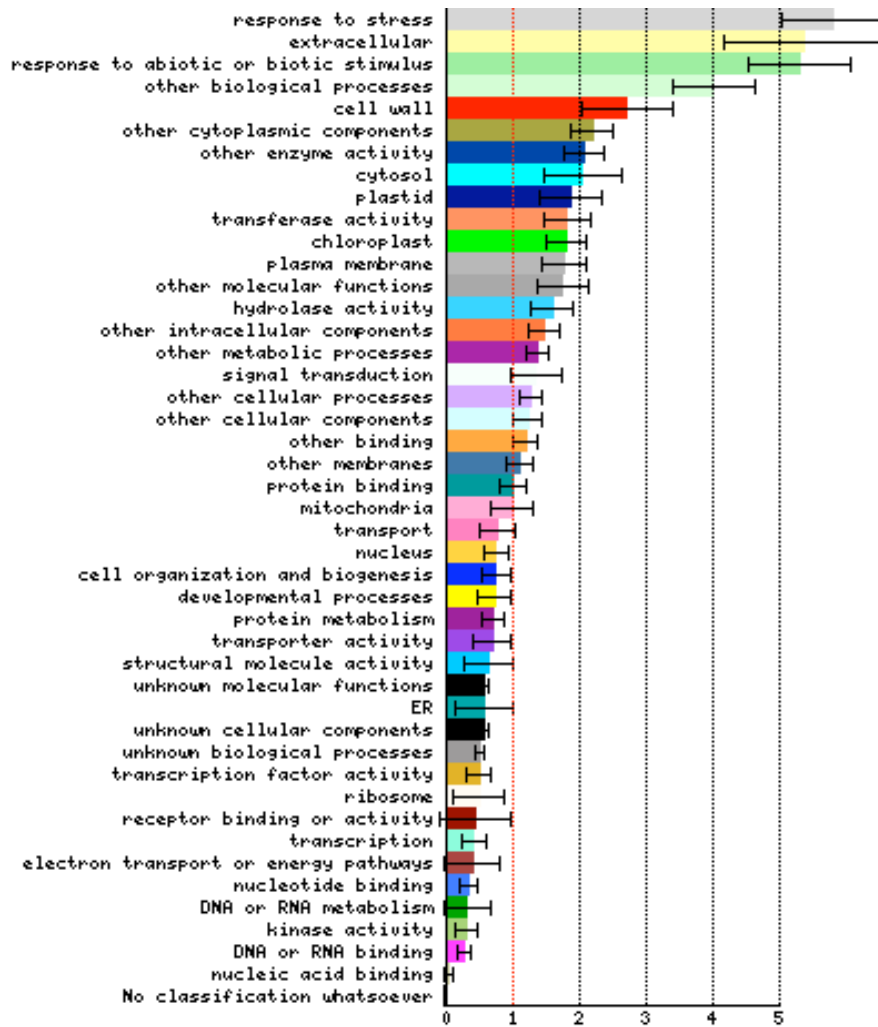
Supplemental Figure 13 : Frequency of functional classes in the genes down-regulated in *lst8-1* mutants grown in short-day conditions and compared to WT plants grown in short days. Results have been obtained from the BAR site (http://bar.utoronto.ca) using the classification SuperViewer. The input set has been bootstrapped 100 times to estimate the reliability of the data. The resulting mean values are shown together with standard deviations.
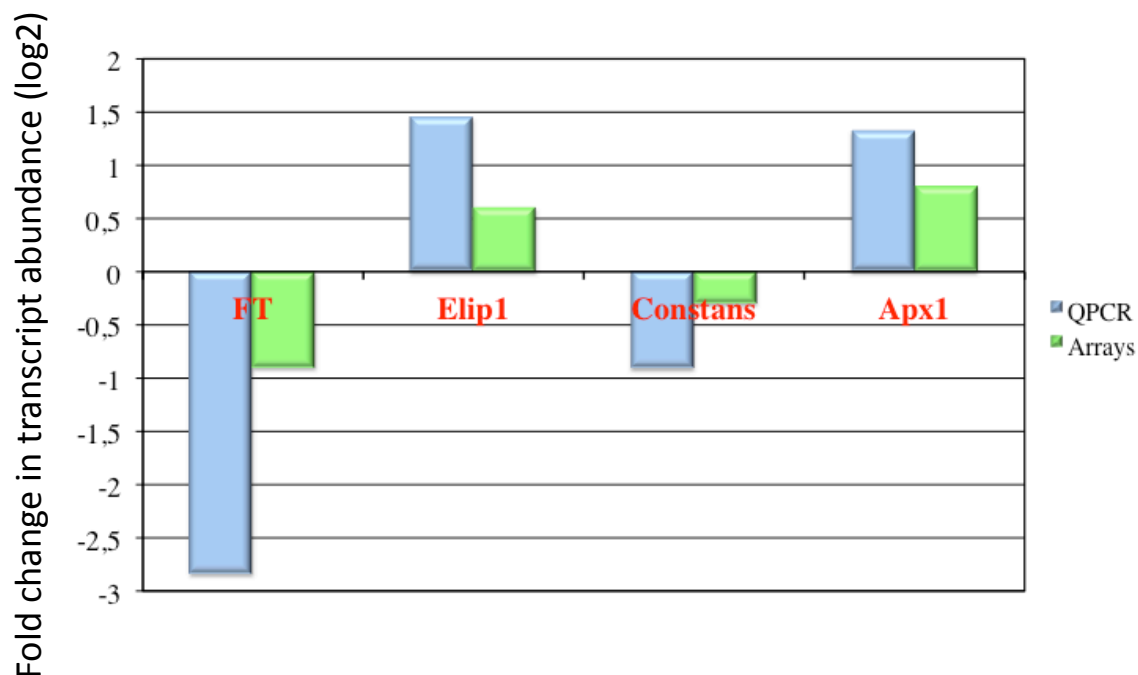
Supplemental Figure 14 : Changes in transcript abundance determined by either quantitative real-time RT-PCR (QPCR) or microarray hybridizations.

Leaves from the *lst8-1* mutant lines were collected after transfer to long-day conditions for 2 days and relative changes in transcript abundance were measured for the indicated genes (see Figure 13 for details). Gene-specific primers for RT-PCR amplification are the ones used for the mirco-arrays gene-specific tag (GST) amplification (see Methods for details and http://urgv.evry.inra.fr/projects/FLAGdb++ for the corresponding sequences).

FT: Flowering locus T

Elip1: Early light-induced protein 1

Apx1: Ascorbate peroxydase 1
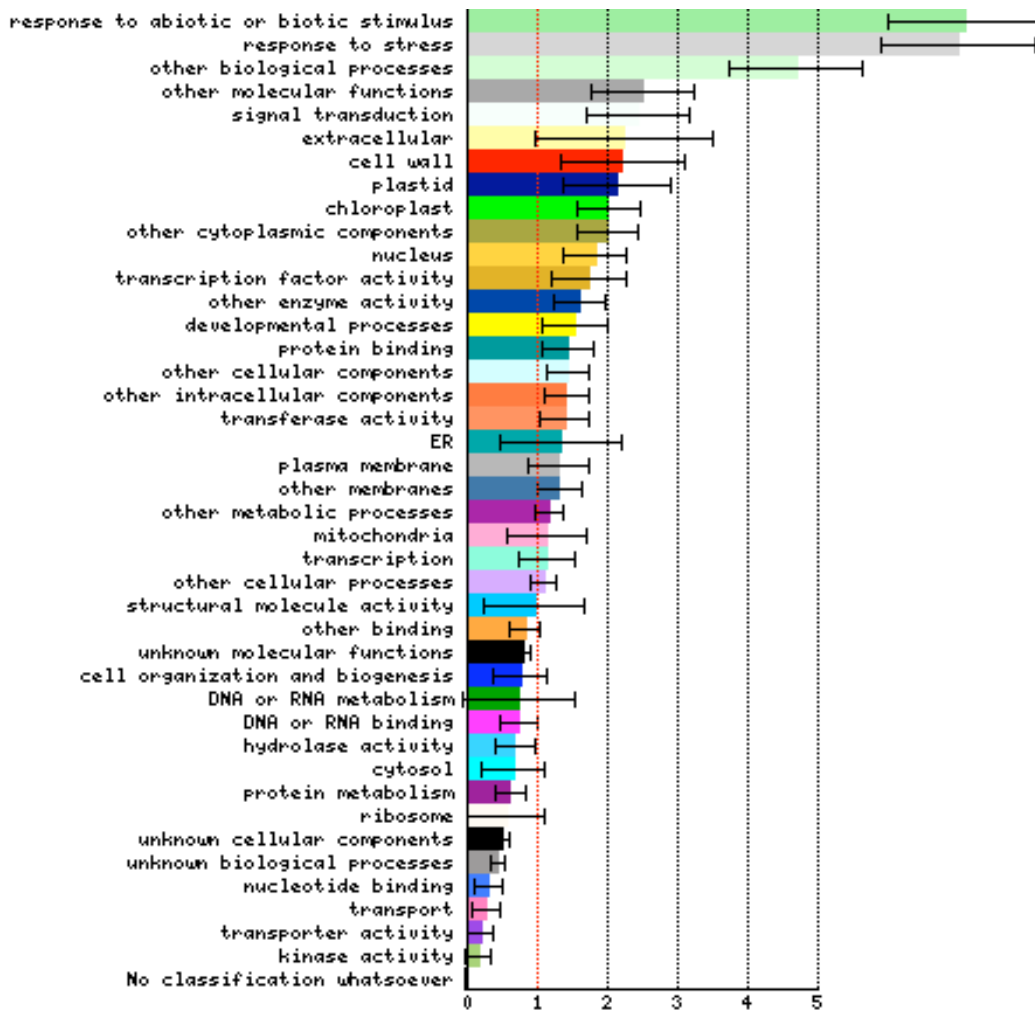
Supplemental Figure 15: Frequency of functional classes in the genes down-regulated in *lst8-1* mutants
after two days under long-day conditions when compared to WT plants grown in the same
conditions.
Results have been obtained from the BAR site (http://bar.utoronto.ca) using the classification
SuperViewer. The input set has been bootstrapped 100 times to estimate the reliability of the data.
The resulting mean values are shown together with standard deviations.
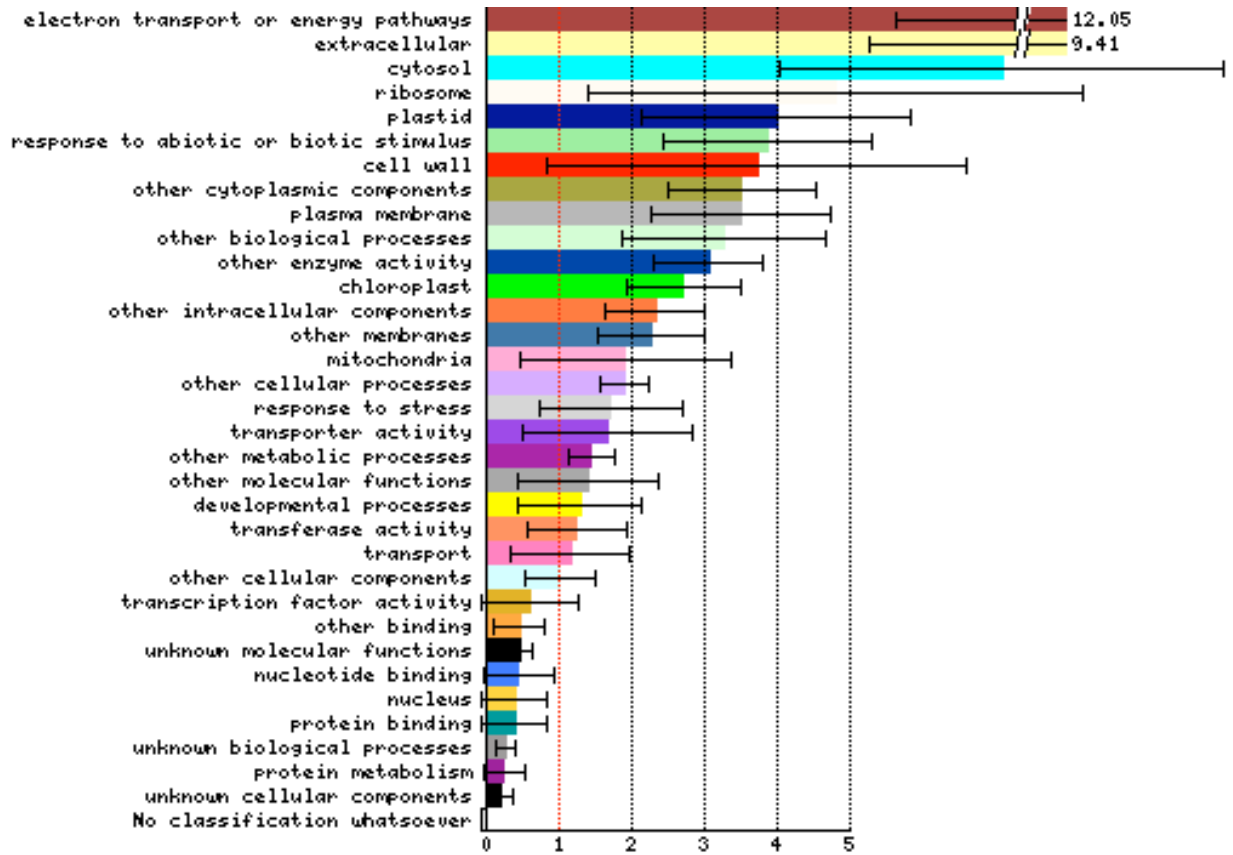
Supplemental Figure 16 : Frequency of functional classes in the genes up-regulated in *lst8-1* mutants
 after two days in long-day conditions when compared to WT plants grown in the same
conditions.
Results have been obtained from the BAR site (http://bar.utoronto.ca) using the classification
SuperViewer. The input set has been bootstrapped 100 times to estimate the reliability of the data.
The resulting mean values are shown together with standard deviations.

LST8-1 (At3g18140)	SALK 02459	02459-F	AGG AGA GGA TGA AGA AAA CGG	Genotyping
		02459-R	TTG CTT CCT TCT ACC TGC TTG	
LST8-1 (At3g18140)	SAIL 641D10	02459-R	TTG CTT CCT TCT ACC TGC TTG	
		LST8 1-R	CAG TGG CTT TGT GAT GAC CTT	
T-DNA primer	SALK line	Lba-1	TGG TTC ACG TAG TGG GCC ATC G	
	SAIL line	LB3-SAIL	TAG CAT CTG AAT TTC ATA ACC AAT CTC GAT ACA C	
LST8-1 (At3g18140)		LST8-18140-5'	ATC GAT CGA AAA TGA GTC AGC	RT-PCR
		LST8-18140-3'	CTT ATT AAG GTT TTA ATC GTG A	
LSt8-2 (At2g22040)		LST8-22040-5'	ACA AAC CGG ATG ATA GTC CC	RT-PCR
		LST8-22040-3'	ACA GGA TTT AAT CAC GCA GT	
LST8-1 (At3g18140)		LST8-1 F	GTT TGG GAC TGC GTC TTC TC	Quanti tati ve RT PCR
		LST8-18140-3'	CTT ATT AAG GTT TTA ATC GTG A	

LST8-1	1kb promoter forward with *EcoRI* site	ATG AAT TCG ATA GAA CAG AGG TTA AGA AC
LST8-1	1kb promoter reverse with *NotI* site	ATT AGC GGC CGC TTT CGA TCG ATT TTA TCC CG
LST8-1	1 kb promoter forward with *BamHI* site	CGG GAT CCG ATA GAA CAG AGG TTA AGA AC
LST8-1	Gene 3' end with *NotI* site	TGC TGC GGC CGC AGG TTT TAA TCG TGA AGT GC
LST8-1	Start of coding sequence with *SalI* site	CGA AGT CGA CTA TGA GTC AGC CTT CT
LST8-1	Start of coding sequence with *EcoRI* site	AGG AAT TCA CCA TGA GTC AGC CT
LST8-1	End of coding sequence with *NotI* site	TGC TGC GGC CGC TTT AAA TCG TGA AG

Supplemental Table 1 : Primer sequences